ARCHIVES OF ELECTRICAL ENGINEERING VOL. 70(4), pp. 743–757 (2021)

DOI 10.24425/aee.2021.138258

Surrogate synthesis of excitation systems for frame tangential eddy current probes

VOLODYMYR YAKOVYCH HALCHENKO, RUSLANA VOLODYMYRIVNA TREMBOVETSKA, VOLODYMYR VOLODYMYROVYCH TYCHKOV

Cherkasy State Technological University
Ukraine

e-mail: halchvl@gmail.com, r.trembovetska@chdtu.edu.ua, v.tychkov@chdtu.edu.ua

(Received: 01.02.2021, revised: 19.04.2021)

Abstract: Existing scientific studies devoted to the design of eddy-current probes with a priori given configuration of the electromagnetic excitation field, which provide a uniform eddy current density distribution, consider a wide class of such, but are limited to the case when the probe is stationary relative to the testing object. Therefore, the actual problem is the synthesis of moving tangential eddy current probes with a frame excitation system that provides a uniform eddy current density distribution in the testing object, the solution of which is proposed in this study.

A mathematical method for nonlinear surrogate synthesis of excitation systems for frame moving tangential surface eddy current probes, which implements a uniform eddy current density distribution of the testing zone object, is proposed. A metamodel of the volumetric structure of the excitation system of the frame tangential eddy current probe, applied in the process of surrogate optimal parametric synthesis, has been created. The examples of nonlinear synthesis of excitation systems using modern metaheuristic stochastic algorithms for finding the global extremum are considered. The numerical results of the obtained solutions of the problems are presented. The efficiency of the synthesized structures of excitation systems in comparison with classical analogs is shown on the graphs of the eddy current density distribution on the object surface in the testing zone.

Key words: additive neural network regression, eddy current probe, stochastic optimization algorithm, surrogate optimization, uniform eddy current density distribution, velocity effect

1. Introduction

Surface eddy current probes (SECPs) are widely used in a flaw detection, including those with automatic scanning objects with the sensor moving along them. At the same time, the requirements for the characteristics of probes in the transition from defectoscopy to defectometry are becoming more stringent. One of these characteristics is the eddy current density (ECD) distribution in the testing object (TO) which predetermines the sensitivity of SECPs to defects. Classical designs of SECPs have a non-uniform ECD distribution in the TO and, accordingly, a non-uniform sensitivity, which affects the detection efficiency and identification of defects.

In recent years scientists have focused their attention on the creation of SECPs with some specific probing properties of the electromagnetic field (EMF), which significantly affect the sensitivity of the ECP. One of these research areas is the provision of an a priori given uniform ECD distribution in the testing zone by special SECP designs [1].

The ideal ECD distribution is its U-shaped form, which can be obtained by various structures of the excitation system (ES), in particular, planar or volumetric, round or rectangular coils, etc. Frame SECPs with rectangular coils are considered better than round ones when detecting defects, since they possess directional properties of EMF and have the ability to create a specific eddy currents distribution. Compared to a conventional flat coil, a rectangular vertical coil can produce a more even eddy currents distribution in an object. The indicated properties and lower sensitivity to oscillations of separation from the TO surface provide advantages for using a rectangular vertical coil as an ES in the process of searching for defects in the form of delamination. Therefore, this paper will focus on the synthesis of tangential frame ECPs, the ES of which provides a uniform ECD distribution.

The researchers in review article [2] and in work [3] analyzed the current trends in the creation of SECPs with various ESs, providing optimal EMF sensing in the testing zone. The published works [1–3] propose ESs, which create a homogeneous EMF of excitation for cases when the TO is stationary. Whereas a similar, but a more complicated problem is not considered for cases of a moving TO. So, it is important to synthesize a moving SECP with an ES, providing a homogeneous ECD distribution in the TO.

The results of the first attempts at optimal surrogate synthesis of a moving circular SECP with planar and volumetric ES structures are presented in [4, 5], and in [6] – a frame SECP with a planar ES structure. The findings of numerical experiments demonstrate the advantages of synthesized ES structures in comparison with classical analogs in meeting the requirements of uniformity. However, in the class of frame, SECPs remain unexplored in terms of the possibility of providing an initially given uniform ECD distribution in the testing zone of the ES with a vertical location of the field-generating source relative to the TO.

The purpose of this research is the creation of a method for the nonlinear surrogate parametric optimal synthesis of ESs of frame moving tangential ECPs with a volumetric structure and a uniform ECD distribution in the testing zone of the object, which is implemented by means of the appropriate metamodel and a stochastic heuristic algorithm for searching for a global extremum.

2. Theoretical part

2.1. Excitation system of a classic moving tangential SECP

Let us consider the ES SECP in the form of a rectangular single turn, located vertically to the TO. The geometric center of the loop is located at a height z_0 above the TO (Fig. 1).

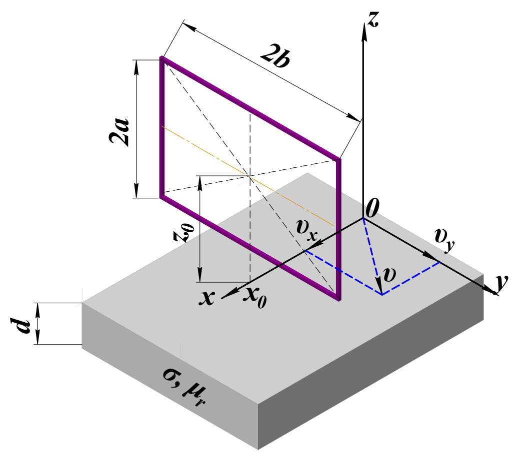

Fig. 1. Frame source of the exciting field in the form of a rectangular loop, located vertically to the TO

Interaction of the field source sounding with the TO is described by the Maxwell system of differential equations. The mathematical model of a single turn of the tangential SECP, developed by researchers and presented in [7, 8], allows us to determine the ECD distribution in the TO under the following assumptions:

- the medium is linear, homogeneous, isotropic;
- the TO is moving, conductive, of an infinite area and has a finite thickness d;
- a rectangular coil with dimensions $a \times b$ is excited by the alternating current I of circular frequency ω;
- the conductor of the excitation source is infinitely thin;
- electrical conductivity σ, relative magnetic permeability μ_r and the velocity vector $\vec{v} = \left(v_x, v_y, 0\right)$ are permanent;
- EMF is quasi-stationary, that is, the displacement current is neglected in comparison with the conduction current as a result of a significantly lower scanning speed compared to the speed of light.

Then, for a quasi-stationary simplification of the EMF representation, Maxwell's equations, which are supplemented by the condition of current continuity, have the form:

$$\begin{aligned} \nabla \times \vec{H} &= \vec{J}, \\ \nabla \times \vec{E} &= -\frac{\partial \vec{B}}{\partial t}, \\ \nabla \cdot \vec{B} &= 0, \\ \nabla \cdot \vec{J} &= 0. \end{aligned} \tag{1}$$

The total current density contains only the conduction current and the transfer current:

$$\vec{J} = \vec{J}_{\text{conduction}} + \vec{J}_{\text{transfer}}, \qquad \vec{J}_{\text{conduction}} = \sigma \cdot \vec{E}, \qquad \vec{J}_{\text{transfer}} = \sigma \cdot \left[\vec{v} \times \vec{B}\right], \tag{2}$$

where: $\vec{H}$ is the vector of the magnetic field intensity; $\vec{E}$ is the vector of electric field intensity; $\vec{B}$ is the vector of magnetic flux density.

The mathematical model was built for several computational domains, the complex values of the magnetic flux density of each were determined:

– in the (1) domain $0 < z < z_0$:

$$\begin{gathered} \vec{B}_1 = \vec{B}_i + \vec{B}_r\,, \\ \vec{B}_i = \nabla \times \vec{A}_i\,, \qquad \vec{A}_i = \frac{\mu_0}{4\pi} \int\limits_l \frac{\vec{J}_{\text{outside}}\, \mathrm{d}l}{R}, \\ \nabla^2 \vec{B}_r = 0, \qquad \nabla \times \vec{B}_r = 0. \end{gathered} \tag{3}$$

where: $\vec{B}_i$ describes the intrinsic magnetic field of a rectangular ES loop with current density $\vec{J}_{\text{outside}}$ and length l; $\vec{A}_i$ is the vector potential; R is the distance from the current source; $\vec{B}_r$ is the magnetic field of eddy currents generated in the medium of the TO; ∇ is the differential operator nabla; $\mu_0 = 4 \times \pi \times 10^{-7}\ \frac{\text{Hn}}{\text{m}}$ is the magnetic constant in vacuum;

– in the (2) domain $-d < z < 0$:

$$\begin{gathered} \nabla^2 \vec{B}_2 - \sigma \cdot \mu_r \cdot \mu_0 \cdot \left(\upsilon_x \cdot \frac{\partial \vec{B}_2}{\partial x} + \upsilon_y \cdot \frac{\partial \vec{B}_2}{\partial y} \right) - j \cdot \omega \cdot \sigma \cdot \mu_r \cdot \mu_0 \cdot \vec{B}_2 = 0, \\ \nabla \cdot \vec{B}_2 = 0, \end{gathered} \tag{4}$$

where $j = \sqrt{-1}$;

– in the (3) domain $z < -d$:

$$\nabla^2 \vec{B}_3 = 0, \qquad \nabla \times \vec{B}_3 = 0. \tag{5}$$

The method of integral Fourier transforms, namely, the direct double transformation was applied to solve partial differential equations in a Cartesian coordinate system:

$$b\,(\xi, \eta, z) = \int\limits_{-\infty}^{\infty} \int\limits_{-\infty}^{\infty} B(x, y, z) \cdot e^{j(x\xi + y\eta)}\, \mathrm{d}x\, \mathrm{d}y, \tag{6}$$

and the inverse double Fourier transformation was used with the obtained images:

$$B(x, y, z) = \frac{1}{4 \cdot \pi^2} \int\limits_{-\infty}^{\infty} \int\limits_{-\infty}^{\infty} b(\xi, \eta, z) \cdot e^{-j(x\xi + y\eta)}\, \mathrm{d}\xi\, \mathrm{d}\eta, \tag{7}$$

where ξ, η are variables of integration.

The analytical solution of equation systems (3)–(5) taking into account the conditions of continuity of the tangential components of the magnetic field intensity $H_{1t} = H_{2t}$ and normal components of magnetic flux density $B_{1n} = B_{2n}$ at the interfaces between the media $z = 0$ and $z = -d$, allowed the authors of [8] to obtain "exact" functional dependences of the distribution of the components of the magnetic flux density B_x, B_y, B_z in the TO medium:

$$B_{2x} = -\frac{\mu_0 \cdot \mu_r \cdot I}{4 \cdot \pi^2} \cdot \int_{-\infty}^{\infty}\int_{-\infty}^{\infty} \frac{\xi^2 \cdot e^{(jx_0 \cdot \xi)}}{\eta \cdot (\xi^2 + \eta^2)} \cdot \frac{\sin(b \cdot \eta)}{(1 - e^{2 \cdot \gamma \cdot d})}$$
$$\cdot \left[\left\{ -(1 + \lambda_0) \cdot e^{2 \cdot \gamma \cdot d} + \nu_0 \cdot e^{-\left(\sqrt{\xi^2+\eta^2} - \gamma\right) \cdot d} \right\} \cdot e^{\gamma \cdot z} + \left\{ 1 + \lambda_0 - \nu_0 \cdot e^{-\left(\sqrt{\xi^2+\eta^2} - \gamma\right) \cdot d} \right\} \cdot e^{-\gamma \cdot z} \right]$$
$$\cdot e^{-z_0 \cdot \sqrt{\xi^2+\eta^2}} \cdot \left(e^{a \cdot \sqrt{\xi^2+\eta^2}} - e^{-a \cdot \sqrt{\xi^2+\eta^2}} \right) \cdot e^{-j(x \cdot \xi + y \cdot \eta)} \, \mathrm{d}\xi \, \mathrm{d}\eta, \tag{8}$$

$$B_{2y} = -\frac{\mu_0 \cdot \mu_r \cdot I}{4 \cdot \pi^2} \cdot \int_{-\infty}^{\infty}\int_{-\infty}^{\infty} \frac{\xi \cdot e^{(jx_0 \cdot \xi)}}{(\xi^2 + \eta^2)} \cdot \frac{\sin(b \cdot \eta)}{(1 - e^{2 \cdot \gamma \cdot d})}$$
$$\cdot \left[\left\{ -(1 + \lambda_0) \cdot e^{2 \cdot \gamma \cdot d} + \nu_0 \cdot e^{-\left(\sqrt{\xi^2+\eta^2} - \gamma\right) \cdot d} \right\} \cdot e^{\gamma \cdot z} + \left\{ 1 + \lambda_0 - \nu_0 \cdot e^{-\left(\sqrt{\xi^2+\eta^2} - \gamma\right) \cdot d} \right\} \cdot e^{-\gamma \cdot z} \right]$$
$$\cdot e^{-z_0 \cdot \sqrt{\xi^2+\eta^2}} \cdot \left(e^{a \cdot \sqrt{\xi^2+\eta^2}} - e^{-a \cdot \sqrt{\xi^2+\eta^2}} \right) \cdot e^{-j(x \cdot \xi + y \cdot \eta)} \, \mathrm{d}\xi \, \mathrm{d}\eta, \tag{9}$$

$$B_{2z} = -j\frac{\mu_0 \cdot \mu_r \cdot I}{4 \cdot \pi^2} \cdot \int_{-\infty}^{\infty}\int_{-\infty}^{\infty} \frac{\xi \cdot e^{(jx_0 \cdot \xi)}}{\gamma \cdot \eta} \cdot \frac{\sin(b \cdot \eta)}{(1 - e^{2 \cdot \gamma \cdot d})}$$
$$\cdot \left[\left\{ -(1 + \lambda_0) \cdot e^{2 \cdot \gamma \cdot d} + \nu_0 \cdot e^{-\left(\sqrt{\xi^2+\eta^2} - \gamma\right) \cdot d} \right\} \cdot e^{\gamma \cdot z} - \left\{ 1 + \lambda_0 - \nu_0 \cdot e^{-\left(\sqrt{\xi^2+\eta^2} - \gamma\right) \cdot d} \right\} \cdot e^{-\gamma \cdot z} \right]$$
$$\cdot e^{-z_0 \cdot \sqrt{\xi^2+\eta^2}} \cdot \left(e^{a \cdot \sqrt{\xi^2+\eta^2}} - e^{-a \cdot \sqrt{\xi^2+\eta^2}} \right) \cdot e^{-j(x \cdot \xi + y \cdot \eta)} \, \mathrm{d}\xi \, \mathrm{d}\eta, \tag{10}$$

where B_{2x}, B_{2y}, B_{2z} are the components of the magnetic flux density in spatial coordinates for domain (2); $\gamma = \sqrt{\xi^2 + \eta^2 - j \cdot \sigma \cdot \mu_0 \cdot \mu_r \cdot \left(\upsilon_x \cdot \xi + \upsilon_y \cdot \eta\right) + j \cdot \omega \cdot \sigma \cdot \mu_0 \cdot \mu_r}$,
$$\lambda_0 = \frac{\left\{\gamma^2 - \mu_r^2 \cdot \left(\xi^2 + \eta^2\right)\right\} \cdot \left(1 - e^{-2 \cdot \gamma \cdot d}\right)}{\left(\gamma + \mu_r \cdot \sqrt{\xi^2 + \eta^2}\right)^2 - \left(\gamma - \mu_r \cdot \sqrt{\xi^2 + \eta^2}\right)^2 \cdot e^{-2 \cdot \gamma \cdot d}},$$
$$\nu_0 = \frac{4 \cdot \mu_r \cdot \gamma \cdot \sqrt{\xi^2 + \eta^2} \cdot e^{\left(\sqrt{\xi^2+\eta^2} - \gamma\right) \cdot d}}{\left(\gamma + \mu_r \cdot \sqrt{\xi^2 + \eta^2}\right)^2 - \left(\gamma - \mu_r \cdot \sqrt{\xi^2 + \eta^2}\right)^2 \cdot e^{-2 \cdot \gamma \cdot d}}.$$

The mathematical model of the ECD distribution within the TO is determined through the partial derivatives of the components of the magnetic flux density (8)–(10) with respect to spatial coordinates x, y, z:

$$\begin{aligned} J_x &= \frac{1}{\mu_0 \cdot \mu_r} \cdot \left[\frac{\partial B_{2z}}{\partial y} - \frac{\partial B_{2y}}{\partial z}\right], \\ J_y &= \frac{1}{\mu_0 \cdot \mu_r} \cdot \left[\frac{\partial B_{2x}}{\partial z} - \frac{\partial B_{2z}}{\partial x}\right], \\ J_z &= \frac{1}{\mu_0 \cdot \mu_r} \cdot \left[\frac{\partial B_{2y}}{\partial x} - \frac{\partial B_{2x}}{\partial y}\right]. \end{aligned} \tag{11}$$

To verify Formulas (11) of the "exact" mathematical model and to analyze the ECD distribution inside the TO using a single round of excitation of a rectangular shape, numerical modeling was carried out for the case of variation of the spatial coordinates $J_{\text{turn}} = f(y, z)$ (Fig. 2), where J_{turn} is the ECD module, and other parameters are fixed. The following initial data were used for the calculation: $\upsilon = (0, 40, 0)$ m/s; $z = -0.5, \ldots, 0$ mm, $y = -25, \ldots, 25$ mm, $a = 16$ mm, $b = 16$ mm; the thickness of conductive material $d = 10$ mm; the height of the location of the center of the loop above the TO $z_0 = 19$ mm; the displacement of the turn from the origin $x_0 = 0$ mm; the electrophysical parameters of the TO material $\sigma = 7.69 \times 10^6$ S/m, $\mu_r = 700$, frequency $f = 4$ kHz, excitation current $I = 1$ A. Multiple integrals in (6), (7) are calculated by the truncation method using Gauss–Konrad quadratures.

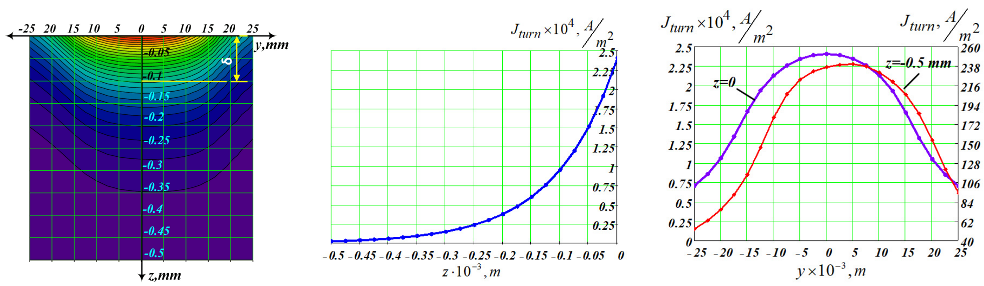

Fig. 2. Level lines and graphs of the ECD distribution inside the TO, created by a single rectangular loop

The conditional depth of eddy current penetration can be theoretically estimated by the formula:

$$\delta = \frac{1}{\sqrt{\pi \cdot f \cdot \mu_r \cdot \mu_0 \cdot \sigma}}\,. \tag{12}$$

For the given initial data, it is 0.1 mm. The comparison with the data of numerical calculations (Fig. 2) makes it possible to assert their adequacy: $J_{z=0} = 2.516 \times 10^4$ A/m²; $J_{z=0.1}9.986 \times 10^3$ A/m²; $J_{z=0}/J_{z=0.1} = 2.52 \approx 2.71$, which corresponds to theoretical concepts.

2.2. Designs of tangential SECP

For further research, it is necessary to consider possible design options for tangential SECPs, differing in the location of the pick-up coil probe (Fig. 3). This is important, because its orientation in space determines which components of the ECP J_x, J_y or J_z form a magnetic flux penetrating the coil loop. In the first version (Fig. 3(a)), the measuring coil of the probe is located in the X0Y plane

$$J = \sqrt{|J_x|^2 + \left|J_y\right|^2},$$

in the second (Fig. 3(b)), it is in the Y0Z plane

$$J = \sqrt{\left|J_y\right|^2 + |J_z|^2},$$

in the last version (Fig. 3(c)) – in the X0Z plane

$$J = \sqrt{|J_x|^2 + |J_z|^2}\,.$$

The so-called biorthogonal versions of SECP designs are also possible, where two measuring coils are used simultaneously, located in the X0Z and X0Y planes, and others. Herewith, the ES remains the same for all variants. It is a rectangular coil with a vertical position relative to the TO.

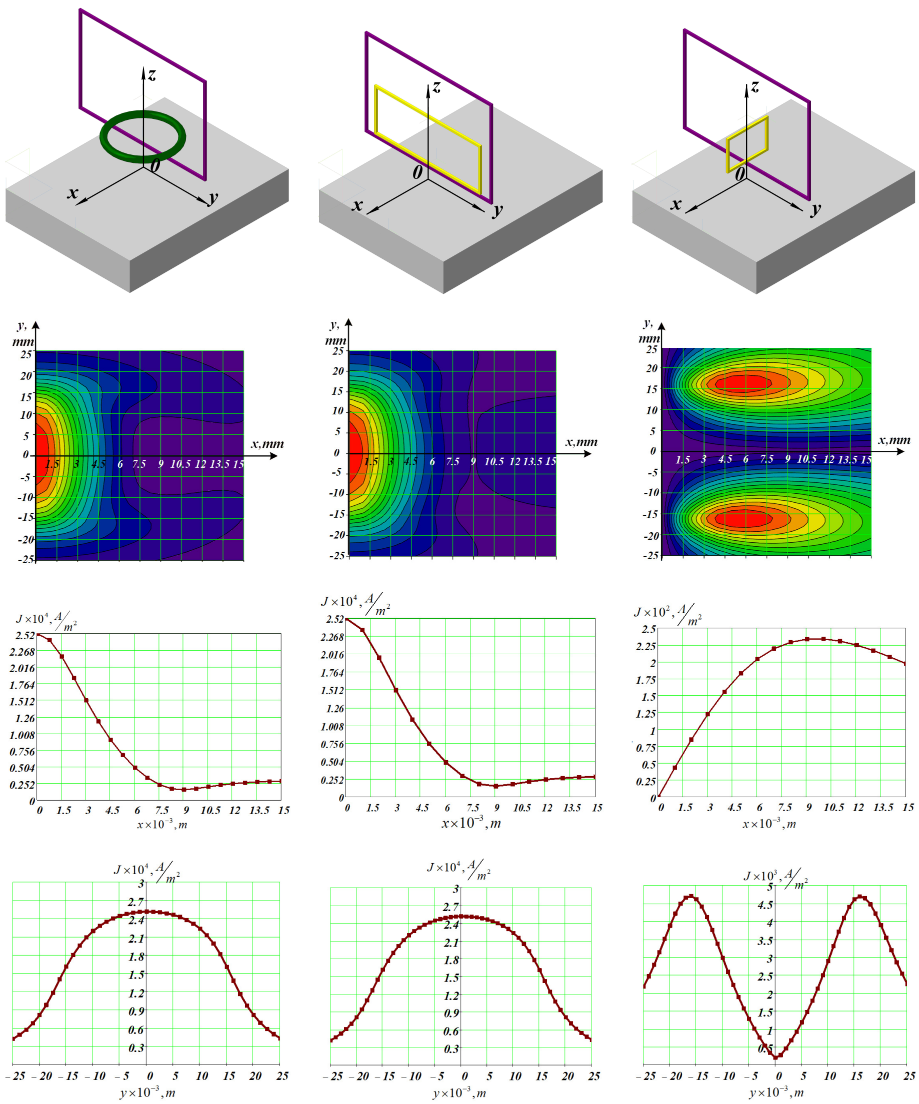

(a) (b) (c)

Fig. 3. ECD distribution in the form of level lines and graphs of their change along the 0X and 0Y axes for the presented structures of tangential SECPs

In Fig. 3, in addition to the variants of the schematic arrangement of the SECP coils, the calculated ECD distributions are also presented in the form of level lines and graphs of their change along the axes 0X and 0Y. In this case, for all variants, the ECD distributions in the X0Y plane on the surface of the TO $z = 0$ are demonstrated.

The tangential design is characterized by the best homogeneity of the ECD distribution among all ES SECPs, but the range of homogeneity is insignificant. For example, for the considered single turn ES with dimensions of 16×16 mm, the range of homogeneity along the 0X axis is about 1 mm, and along the 0Y axis is 8 mm (Fig. 3(a), 3(b)). As a rule, in a static SECP, the homogeneity zone can be significantly expanded by using a rectangular ES coil having a certain length along the 0X axis, that is, by using a source of a uniform EMF. But for the moving SECP, due to the formation of additional eddy currents in the TO, caused by the effect of velocity, it is not entirely acceptable. Therefore, it makes sense to consider a discretized sectioned analogue of such an ES, which is a homogeneous system of rectangular coils, the design parameters of which are determined as a result of optimal synthesis. This approach was successfully applied for the synthesis of the ES circular SECP with planar [9] and volumetric structures and the flat rectangular ES with the generation of a magnetic flux of excitation normal to the TO [6].

2.3. Problem of optimal synthesis of ESs of moving tangential SECP

Optimal design stands for the synthesis of ES SECPs, providing initially given uniform ECD distribution at the testing points of the TO zone. The set of points is put uniformly inside the TO, but in the simple case, it is allowed to set them on its surface. The number of points N determines the accuracy of the ECD distribution. In this research, we restrain to the parametric optimal synthesis of ESs. The structure of an ES is considered to be specified, that is, the number of sections in the ES is predetermined. We will consider a tangential SECP with a rectangular volumetric structure ES, which is a set of M sectional coils, each containing w and $(i = 1, \ldots, M)$ turns. All coils are powered by alternating current I of circular frequency ω, electrically connected in series, and are wound sequentially-oppositely or sequentially-according to different MMF Iw_i they have. This rectangular volumetric structure of ES is characterized by the sectional coils with geometric dimensions of the sides $2a_i \times 2b_i$ of each of them and displacements x_{0i} and coils relative to each other from the origin of the coordinate system along the 0X axis (Fig. 1). Subsequently, square sections were used for numerical experiments. The position of the coils is also determined by the heights z_{0i} of their location above the TO. In this study, the height for all sections is constant and equals z_0. As a result of nonlinear synthesis, the geometric dimensions of all coils $2a_i$, their displacements x_{0i} and MMF Iw_i are determined.

The synthesis problem is formulated in the optimization setting [10]. The objective function is presented in the form of a quadratic functional:

$$F_{\text{target}} = \sum_{i=1}^{N} \left(\sum_{k=1}^{M} J_{ik} - J_{\text{reference}} \right)^2 \to \min, \tag{13}$$

where: $J_{\text{reference}}$ is the initial value of the ECD module at the testing point; J_{ik} is an ECD module at the TO testing point with number i, created by the k_{th} coil of the ES SECP.

The form of the ECD distribution in the TO is effective for problems of defectometry with the maximum localization and concentration in the testing zone, while outside the ECD it has a zero value. It is this form of distribution that is taken as an initially given for the synthesis problem. The problem solution of ES synthesis using the "exact" electrodynamic model (8)–(11) is not possible due to its significant computational resource intensity [11]. Reducing the time for calculating the objective function is achieved by using a metamodel [12, 13], that is, a substitute model, which has a high computational performance and makes it possible to find a solution to the problem by means of surrogate optimization techniques in real time. This approach has already been used to solve the problems of the synthesis of SECPs of planar and volumetric structures with different geometries of ES coils [4–6, 9].

Within the framework of this approach, it is first supposed to construct a metamodel of a framework tangential SECP. The ECD distribution for a moving tangential SECP in the technique of the surrogate modeling is described by a four-dimensional approximation dependence $\hat{J} = f(x, y, a, x_0)$, where x and y are spatial coordinates on the TO surface in the testing zone.

The creation of a multiparametric approximation model was carried out on the basis of neural networks (NN) on radial basis functions [14, 15]. Due to a hybrid approach, namely, additive NN-regression applying network committees at each of its levels and decomposition of the search space into several subdomains, it was possible to obtain metamodels with an acceptable approximation error. A committee of networks with decision-making by averaging over the ensemble [5, 6, 9, 16] was applied at each intermediate level of additive NN-regression.

Building a multidimensional metamodel with neural network tools provides for training the network on a data sample. Subsamples for training, testing, and testing of the reproducibility of the response hypersurface were generated using the running procedure. In this case, a computer method for planning an experiment with highly homogeneous filling of a multidimensional search space with nodal points was applied [17], since it better provides reproduction of a global and local behavior of the response surface. An effective four-dimensional computer design of the experiment with low values of centered $CD_4 = 4.14 \times 10^{-6}$ and wrap-around $WD_4 = 6.32$ discrepancies for $N_{\text{training}} = 2500$ [18], is implemented on the basis of combinations of quasi-random Sobol's LP_τ-sequences $(\xi_1, \xi_2, \xi_3, \xi_5)$. The array of initial data with the number of points N_{training} was created for four parameters, varying within: $x = 0, \ldots, 15$ mm, $y = -25, \ldots, 25$ mm, $a = 4, \ldots, 16$ mm, $x_0 = 0, \ldots, 4$ mm, for which the ECD distribution is calculated according to functional dependencies (8)–(11). All other parameters were considered constant. The search area by coil size a was divided into six sub-domains: $4 \leq a < 6$ mm, $6 \leq a < 8$ mm, $8 \leq a < 10$ mm, $10 \leq a < 12$ mm, $12 \leq a < 14$ mm, $14 \leq a \leq 16$ mm.

Additive NN-regression assumes its construction at several intermediate levels, the number of which depends on the value of the approximation error (relative average error *MAPE*, %). In the given model examples, it did not exceed 5%. As a result of such a hybrid construction of additive NN-regression, it was possible to obtain, at a certain stage of its training, the *MAPE* value for local ECD distributions at a level from 2.14% to 4% for each of the subdomains. The verification of the created metamodel was carried out by checking the correctness of the reproducibility of the response hypersurface in the entire modeling area at a significantly larger number of points $N_{\text{reconstitution}} = 4090$. Therefore, the obtained metamodel is correct and ensures the reproduction of the response surface with the maximum error *MAPE* 4.47%. In addition, the resulting metamodel was assessed both at the training stage and at the stage of reproduction, also by a number of statistical quantitative indicators and some qualitative ones [19], in particular, the adequacy of the constructed surrogate model was checked with the help of the Fisher criterion, and its information content was checked by means of coefficient of determination.

The search for the global extremum of functional (13) was carried out using stochastic algorithms, which are well proven in solving nonlinear inverse problems [20, 21]. Therefore, they were used to solve the problem of conditional optimization with the restrictions indicated earlier. The best solution results are obtained by several algorithms. This is a hybrid algorithm based on the genetic search with a local search using the Nelder-Mead simplex method, a PSO-RND particle swarm algorithm with a random link topology strategy and a population metaheuristic optimization algorithm with a swarm of particles with the evolutionary formation of the swarm composition, which is a low-level hybridization of the genetic algorithm and the PSO algorithm [22–24].

3. Numerical experiments of surrogate synthesis of ES

Numerical experiments were carried out for volumetric structures of the ES of tangential SECP with a different number of sectional coils $M = 2{-}5$. As a result of the preliminary analysis, several variants of ES designs were selected, characterized by the best approximation of the ECD distributions to a uniform one, which cover the area in the testing zone with the approximate dimensions along the 0X axis $l_x = 5$ mm and along axes 0Y — $l_y = 24$ mm. The numerical results of solving the synthesis problems are presented in Table 1.

Table 1. Results of surrogate synthesis of ES of frame tangential SECP
with various variants of volumetric structures

No.	Synthesized excitation systems					
	$M = 2$			**$M = 3$**		
	a (mm)	x_0 (mm)	Iw (A × turns)	a (mm)	x_0 (mm)	Iw (A × turns)
1	6.9	2.23	–32.14	7	3.13	–26.96
2	11.77	1.88	11.23	8.74	1.29	15.38
3				15.92	2.6	1.54

No.	Synthesized excitation systems					
	$M = 4$			**$M = 5$**		
	a (mm)	x_0 (mm)	Iw (A × turns)	a (mm)	x_0 (mm)	Iw (A × turns)
1	7.64	1.19	–27.94	5.46	4	–19.59
2	12	2.17	2.55	8.34	1.18	–100
3	12.56	1.15	9.5	8.34	1.05	100
4	15.1	3.84	–0.33	9.56	1.6	20.09
5				5.45	0	–33.57

Figure 4(a) shows the synthesized ECD distributions for ES structures with the number of sectional coils from two to five in the form of level lines. The calculation of the ECD $J = \sqrt{|J_x|^2 + \left|J_y\right|^2}$ distributions was carried out for ES with the parameters obtained as a result

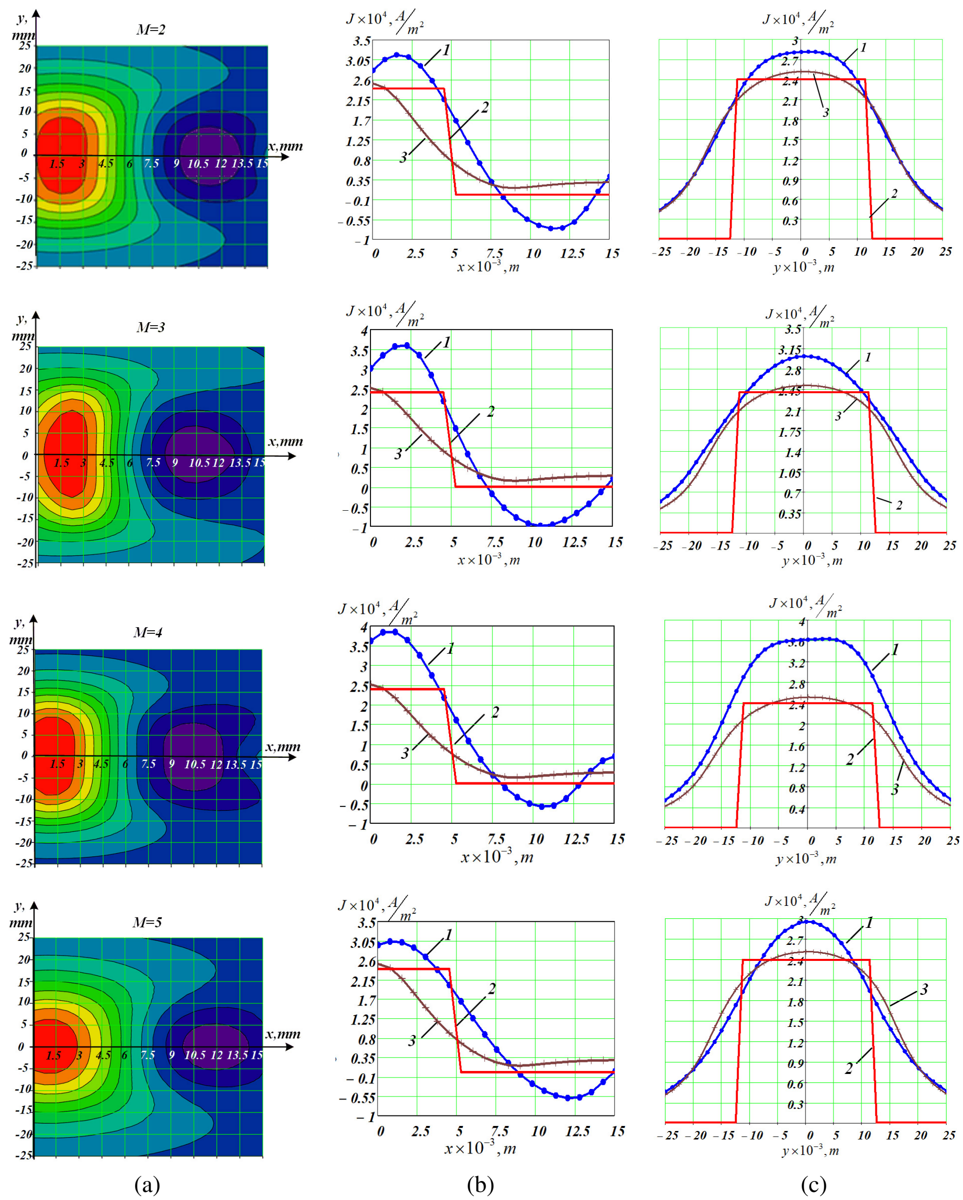

Fig. 4. The results of optimal surrogate synthesis of volumetric structures of ES of moving frame tangential SECP: (a) lines of the level of distributions of AVP; (b) ECD distribution along the 0X axis; (c) ECD distribution along the 0Y axis

of the synthesis according to the “exact” electrodynamic model (dependence 1). Graphs of their behavior along the axes 0X and 0Y are shown in Fig. 4(b) and 4(c), respectively. For comparison purposes, the same figures show the desired ECD distribution (dependence 2) and the distribution created by a single square turn with dimensions of 16×16 mm (dependence 3).

The designs of the synthesized ESs probes with the obtained geometric parameters of the coils, MMF and positioning coordinates on the 0X axis are shown schematically in Fig. 5.

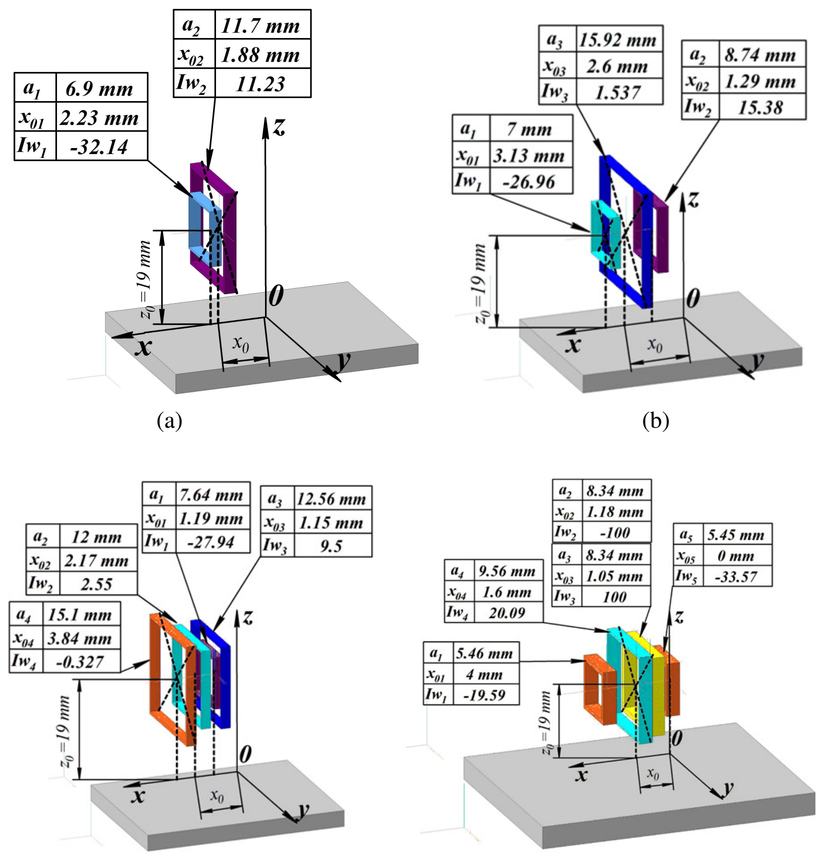

(a) (b)

(c) (d)

Fig. 5. Schematic representation of the coils’ ES arrangements: (a) $M = 2$; (b) $M = 3$; (c) $M = 4$; (d) $M = 5$

4. Discussion

All synthesized ES structures presented in Table 1 implement a close to uniform ECD distribution, which exceeds the given intensity level $J_{\text{reference}} = 2.41$ A/m^2 on the site $0 < x < 5$ mm and $-12 < y < 12$ mm. It is illustrated in Fig. 4(a). It does not appear to be a disadvantage, but on the contrary, can be considered to be a merit. In addition, a comparison of the ECD distributions, created by the synthesized bulk structures of the ES and a single turn of a square shape, indisputably indicates that all the synthesized variants have better results. This is convincingly evidenced by the graphical dependences 1, 2 and 3 in Fig. 4(b), 4(c).

A design variant of the ES SECP with $M = 5$ can be considered an unacceptable from a technical point of view. Sections 2 and 3 of this ES actually compensate for each other's excitation fields, generated by them. The geometrical dimensions and displacements along the 0X axis of the sectional coils are numerically the same, while the MMFs are characterized by the same and opposite values. That is, this ES structure can be considered redundant. The structures of the ES with $M = 3$ and $M = 4$ are comparable in terms of expediency of application. They are equivalent in terms of the total number of ampere-turns required to create an ES. However, the ES variant with $M = 4$ is more complicated in the technological sense. Firstly, it is characterized by a large number of sections. Secondly, sections 1 and 3 of this ES are placed at the same position on the 0X axis. Although they are different in geometric dimensions, it causes certain difficulties in the manufacture of ESs.

With almost the same results in ensuring a uniform ECD distribution, preference should be given to a simple in technical implementation ES structure with $M = 2$ sectional coils.

The results of model calculations on the creation of optimal ESs of a volumetric structure for tangential moving frame SECPs testify to the effectiveness of the proposed method of surrogate parametric synthesis, which ensures a uniform ECD distribution inside the TO and guarantees a uniform sensitivity of probes to defects.

5. Conclusions

The study proposes a method of surrogate nonlinear parametric synthesis of a moving frame tangential SECP with a volumetric structure of the ES, which provides a close to uniform ECD distribution on the surface in the testing zone of the object. This fact accordingly contributes to an efficient process of detecting and identifying defects due to the uniform sensitivity of the SECP.

To implement the proposed method, software has been developed for calculating the direct problem of electrodynamics using an "exact" mathematical model. A software generator of multidimensional computer plans of experiments has been created based on combinations of quasi-random Sobol's LP_τ-sequences with low divergence indices. These designs implement a homogeneous filling of the search space with nodal points for constructing an approximation surrogate model of the response hypersurface. A four-dimensional ES metamodel of a moving tangential SECP was constructed using additive NN-regression. An acceptable error of the metamodel is ensured through the use of NN committees at each intermediate level of additive NN-regression and the search domain decomposition method. Numerical experiments have proved the effectiveness of the proposed means of optimal design of the ES SECP.

References

[1] Repelianto A.S., *Development of uniform eddy current probes using multi excitation coils*, Doctoral Dissertation, Graduate School of Environment and Information Sciences, Yokohama National University (2020).

[2] Halchenko V.Y., Trembovetskaya R.V., Tychkov V.V., *Surface eddy current probes: excitation systems of the optimal electromagnetic field (review)*, Devices and Methods of Measurements, vol. 11, no. 2, pp. 91–104 (2020), DOI: 10.21122/2220-9506-2020-11-2-91-104.

[3] Huang L., Zou J., Zhang J., Zhou Y., Deng F., *A novel rectangular vertical probe with a conductive shell for eddy current testing*, International Journal of Applied Electromagnetics and Mechanics, vol. 62, no. 1, pp. 191–205 (2019), DOI: 10.3233/JAE-190058.

[4] Halchenko V.Y., Trembovetskaya R.V., Tychkov V.V., *Linear synthesis of non-axial surface eddy current probe*s, International Journal "NDT Days", vol. 2, no. 3, pp. 259–268 (2019).

[5] Trembovetska R.V., Halchenko V.Y., Tychkov V.V., Storchak A.V., *Linear synthesis of uniform anaxial eddy current probes with a volumetric structure of the excitation system*, International Journal "NDT Days", vol. 3, no. 4. pp. 184–190 (2020).

[6] Trembovetska R.V., Halchenko V.Y., Tychkov V.V., Bazilo C.V., *Linear synthesis of frame eddy current probes with a planar excitation system*, International Scientific Journal "Mathematical Modeling", vol. 4, no. 3. pp. 86–90 (2020).

[7] Itaya T., Ishida K., Kubota Y., Tanaka A., Takehira N., *Visualization of eddy current distributions for arbitrarily shaped coils parallel to a moving conductor slab*, Progress in Electromagnetics Research M, vol. 47, pp. 1–12 (2016), DOI: 10.2528/pierm16011204.

[8] Itaya T., Ishida K., Tanaka A., Takehira N., Miki T., *A new analytical method for calculation of eddy current distribution and its application to a system of conductor-slab and rectangular coil*, Progress in Electromagnetics Research Symposium, pp. 135–139 (2011).

[9] Halchenko V.Y., Trembovetska R.V., Tychkov V.V., Storchak A.V., *Nonlinear surrogate synthesis of the surface circular eddy current probes*, Przegląd Elektrotechniczny, no. 9, pp. 76–82 (2019), DOI: 10.15199/48.2019.09.15.

[10] Halchenko V.Y., Trembovetska R.V., Tychkov V.V., *Development of excitation structure RBF-metamodels of moving concentric eddy current probe*, Electrical Engineering & Electromechanics, no. 2, pp. 28–38 (2019), DOI: 10.20998/2074-272X.2019.2.05.

[11] Trembovetska R.V., Halchenko V.Y., Tychkov V.V., *Studying the computational resource demands of mathematical models for moving surface eddy current probes for synthesis problems*, Eastern-European Journal of Enterprise Technologies, vol. 95, no. 5/5, pp. 39–46 (2018), DOI: 10.15587/1729-4061.2018.143309.

[12] Forrester A.I.J., Sóbester A., Keane A.J., *Engineering design via surrogate modelling: a practical guide*, Chichester, Wiley (2008).

[13] Koziel S., Echeverrı'a-Ciaurri D., Leifsson L., *Surrogate-based methods*, Computational Optimization, Methods and Algorithms, Berlin, Springer-Verlag, pp. 33–59 (2011), https://link.springer.com/chapter/10.1007/978-3-642-20859-1_3

[14] Simon Haykin, *Neural networks: a complete course*, Moscow, Williams Publ. House (2006).

[15] Géron A., *Hands-on machine learning with scikit-learn, keras, and tensorflow*, O'Reilly Media (2019).

[16] Halchenko V.Y., Trembovetska R.V., Tychkov V.V., Storchak A.V., *Methods for creating metamodels: state of the question*, Visnyk of Vinnytsia Politechnical Institute, vol. 151, no. 4, pp. 74–88 (2020), DOI: 10.31649/1997-9266-2020-151-4-74-88.

[17] Elsawah M., *Constructing uniform experimental designs: in view of centered and wrap-around discrepancy*, LAP LAMBERT Academic Publishing: (Theory of probability, stochastics, mathematical statistics) (2014).

[18] Halchenko V.Y., Trembovetska R.V., Tychkov V.V., Storchak A.V., *The construction of effective multidimensional computer designs of experiments based on a quasi-random additive recursive Rd-sequence*, Applied Computer Systems, vol. 25, no. 1, pp. 70–76 (2020), DOI: 10.2478/acss-2020-0009.

[19] Brink H., Richards J., Feverolph M., *Machine learning*, SPb, Peter (2017).

[20] Benchabira A., Khiat M., *A hybrid method for the optimal reactive power dispatch and the control of voltages in an electrical energy network*, Archives of Electrical Engineering, vol. 68, no. 3, pp. 535–551 (2019), DOI: 10.24425/aee.2019.129340.

[21] Kuznetsov B.I., Nikitina T.B., Bovdui I.V., *Active shielding of magnetic field of overhead power line with phase conductors of triangle arrangement*, Technical Electrodynamisc, no. 4, pp. 25–28 (2020), DOI: 10.15407/techned2020.04.025.

[22] Halchenko V.Y., Yakimov A.N., Ostapuschenko D.L., *Global optimum search of functions with using of multiagent swarm optimization hybrid with evolutional composition formation of population*, Information Technology, no. 10, pp. 9–16 (2010).

[23] Halchenko V.Y., Yakimov A.N., Ostapuschenko D.L., *Method of Pareto-optimal parametric synthesis of axially symmetric magnetic systems taking into account the nonlinear magnetic properties of a ferromagnetic*, Journal of Technical Physics, no. 7, pp. 1–7 (2012).

[24] Suresho V., Janiko P., Jasinskio M., *Metaheuristic approach to optimal power flow using mixed integer distributed ant colony optimization*, Archives of Electrical Engineering, vol. 69, no. 2, pp. 335–348 (2020), DOI: 10.24425/aee.2020.133029.